Journal of Theoretical and Applied Mechanics, Sofia, 2005, vol. 35, No. 3, pp. 87–96

# COMBINED FIELDS

## MATHEMATICAL ANALYSIS OF STRESS INDUCED PRESSURE RELAXATION IN OSTEONS

N. Petrov
*Institute of Mechanics, Bulgarian Academy of Sciences,*
*Acad. Bonchev Str., Bl. 4, 1113 Sofia, Bulgaria,*
e-mail: nikolapetrov@dir.bg

[Received 04 August 2005. Accepted 14 November 2005]

Abstract. The objective of the present study is to present a new approach to explaining the experimentally observed relaxation times at stress induced fluid flow in bone. The principle idea is based on the assumptions for fluid exchange between the lacunar-canalicular system and the matrix micro-porosity. The basic difference between the present concept and the concept exploited by Cowin and co-workers (1994, 1995, 1997, 1998, 1999) is in the acceptance of interstitial fluid flow at the micro-structural level. Cowin and co-workers entirely reject the idea of fluid exchange between the lacunar-canalicular porosity and micro-porosity, which is in contradiction with the physiological point that each bone compartment including the micro-porosity should be fluidly acceptable for metabolic exchange processes. On the base of mathematical analysis of anatomical model of Petrov and Pollack (2000) the experimental observation of two relaxation times, at step type bone samples loading, is explained quantitatively for first time in the literature.
Key words: stress induced, fluid flow, bone osteon.

### 1. Introduction

Based on heuristic scheme of Piekarski and Munro (Fig. 1) [1] for osteonal lacunar-canalicular net, Pollack *et al.* [2] developed mathematical model for a system of independent lacunae each connected to Haversian canal with a set of canaliculi. The principle preposition of this model was that effective elastic moduli would be used for describing the interaction between the lacunar fluid and bone matrix and consequently for modelling the canalicular fluid transport. Excellent agreement was found with the experimental

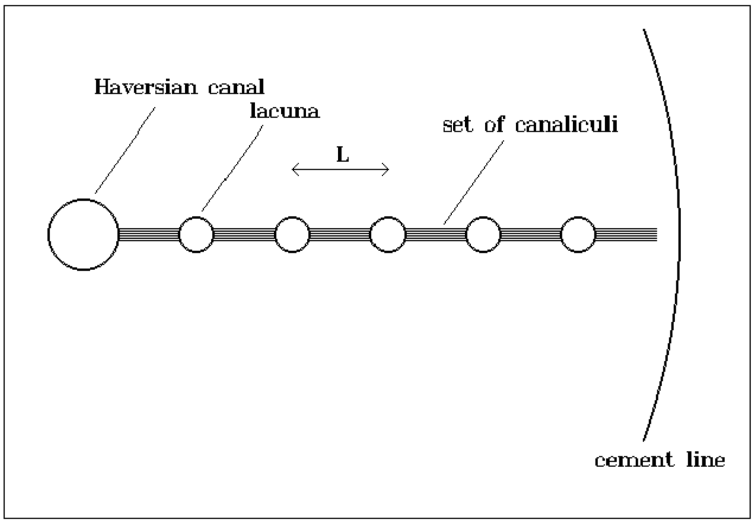


Fig. 1. Shematic osteonial model of Piekarski and Munro

data measured by Pienkowski [3] for samples composed of many osteons. This mathematical model was extended later by Kufahl and Saha, [4] for a series of lacunae and canaliculi as in Piekarski and Munro [1]. Weinbaum *et al.* [5] and Zeng *et al.* [6] used the Kufahl and Saha model introducing a hypothetical existence of a glycocalyx matrix structure within the canaliculus. The presence of the fiber network occupying the inner one half of the radius of the canaliculus with the osteocytic process results in sufficient increased drag to enable this model to predict the experimentally observed order of the relaxation time constant of the order of 1,0 sec. There are, however, some principle problems connected with the Weinbaum *et al.* model. One of them is the assumption that the total water within the micro-porosity compartment is in a frozen state and is not free to flow. They base their argument on Neuman and Neuman's work [7], in which they centrifuged a single synthetic specimen of L-apatite and found that enough water was retained to account for a 100 Angstrom film that accounted for all the bound water. This work, however, was not done on bone. In addition, there is the implicit assumption in Neuman's interpretation that in the bone micro-porosity there are no dead ended pores. The existence of dead ended pores would change tremendously the interpretation of the Neuman experiment. From Newman's model of the porous space in L-apatite and from gas adsorption studies, Weinbaun *et al.* [5] concluded that the water in bone was bound water with thickness of 100 Angstroms. This value is however in absolute conflict with the current conception that for a wide set of materials the shear layer (or slip plane) thickness at the water-solid interface is about 10 Angstroms. The other problem of Weinbaum *et al.* model is the accepted 6 to 7 nM spacing of their glycocalyx. It would "filter" the flow in tracer studies and prohibit the movement of ferritin into the lacunar-canalicular spaces, which will cause serious disagreement with extensive experimental results by many authors (Dillaman, [8]).

## 2. New mathematical model for stress induced fluid flow in osteon at instantaneous loading

To take into account the fluid exchange between the microporosity compartment and lacunar canalicular system Pollack and Petrov [9] extended their model [2] and the model of Kufahl and Saha [4]. The respective master equations are:

$$
(1)\qquad
\begin{aligned}
&\frac{d}{dt}\{P\} + \frac{1}{\hat{\tau}}\,[S]\,\{P\} = \beta\,\frac{\left(\left\{\tilde{P}\right\} - \{P\}\right)}{\tilde{\tau}}, \\
&\frac{d}{dt}\left\{\tilde{P}\right\} = -\frac{\left(\left\{\tilde{P}\right\} - \{P\}\right)}{\tilde{\tau}}, \qquad t \in (0, t_0], \\
&P_0 = -\frac{K_w}{3K_1}\,\frac{4\mu_1 + 3K_1}{4\mu_1 + 3K_w} S, \qquad t = 0, \\
&\hat{\tau} = \frac{8\,\eta\,L\,V_0^{cl}}{n\,\pi\,R_{eff}^4}\,\frac{4\,\mu_1 + 3\,K_w}{4\,\mu_1 K_w}, \\
&\tilde{\tau} = \frac{\eta\,\tilde{V}_0}{C^{exch}}\,\frac{4\,\mu_1 + 3\,K_w}{4\,\mu_1 K_w}, \\
&\beta = \frac{\tilde{V}_0}{V_0^{cl}},
\end{aligned}
$$

where

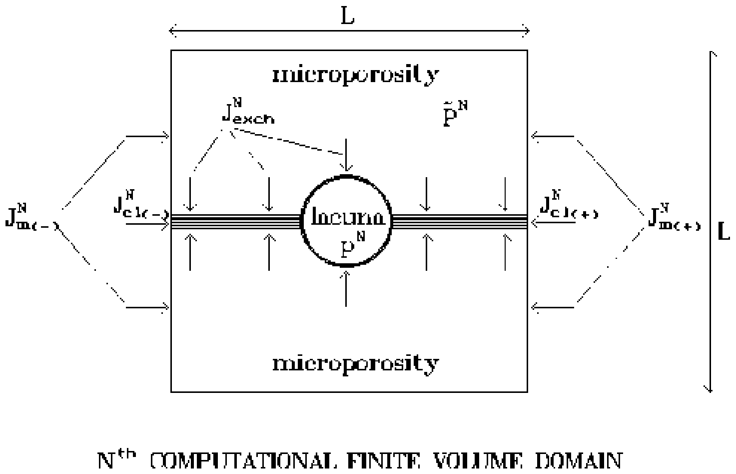


Fig. 2. Scheme of the fluid balance sources in one representative finite volume element ($J_{**}$ exchange fluxes)

$$(2) \qquad [S] \equiv \begin{pmatrix} 2 & -1 & 0 & 0 & . & . & . & 0 & 0 & 0 & 0 \\ -1 & 2 & -1 & 0 & . & . & . & 0 & 0 & 0 & 0 \\ . & . & . & . & . & . & . & . & . & . & . \\ 0 & 0 & 0 & 0 & . & . & . & 0 & -1 & 2 & -1 \\ 0 & 0 & 0 & 0 & . & . & . & 0 & 0 & -1 & 1 \end{pmatrix},$$

$\left\{\tilde{P}\right\}$ and $\{P\}$ are vectors composed by microporosity and lacunar pressures $\tilde{P}^K$ and $P^K$, respectively, for $K$-domain (Fig. 2). The values $V_0^{cl}$, $\tilde{V}_0$, $R_{eff}$, $\eta$, $C^{exch}$, $\mu_1$, $K_1$, $K_w$, $n$, $S$ and $L$ are, respectively, lacunar-canalicular porosity and microporosity volume fractions, effective canalicular radius, canalicular fluid viscosity, ability of the fluid exchange between the lacunar-canalicular and microporosity compartments, effective shear and bulk modulus of bone matrix, bulk modulus of fluid, number of the canalicule in lacunar – canalicular series, uniaxial stress and lacuna to lacuna distance. One can see that the model is dependant on only three parameter combinations, namely – $\hat{\tau}$, $\tilde{\tau}$, $\beta$ (5).

## 3. Relaxation times problem

By eliminating $\left\{\tilde{P}\right\}$ into equations (1) we obtain for lacunar-canalicular pressure

$$\text{(3)} \qquad \frac{d^2}{dt^2}\{P\} + \left(\frac{1}{\hat{\tau}}[S] + \frac{(1+\beta)}{\tilde{\tau}}[I]\right)\frac{d}{dt}\{P\} + \frac{1}{\hat{\tau}\,\tilde{\tau}}[S]\ \{P\} = 0,$$

where $[I]$ is unit matrix.

The formal mathematical solution of the equation (3) and $(1)_2$ is

$$\text{(4)} \qquad \begin{aligned} P_K &= P_0 \sum_{m=1}^{M} C^m \left( \frac{\tau_1^m - \tilde{\tau}}{\tau_1^m - \tau_2^m} \exp\left(-\frac{t}{\tau_1^m}\right) + \right. \\ &\quad \left. + \frac{\tilde{\tau} - \tau_2^m}{\tau_1^m - \tau_2^m} \exp\left(-\frac{t}{\tau_2^m}\right)\right) \sin\frac{(2m-1)K\pi}{(2M+1)}, \\ \tilde{P}_K &= P_0 \sum_{m=1}^{M} C^m \left( \frac{\tau_1^m}{\tau_1^m - \tau_2^m} \exp\left(-\frac{t}{\tau_1^m}\right) - \right. \\ &\quad \left. - \frac{\tau_2^m}{\tau_1^m - \tau_2^m} \exp\left(-\frac{t}{\tau_2^m}\right)\right) \sin\frac{(2m-1)K\pi}{(2M+1)}, \\ K &= 1, 2, \ldots, M, \end{aligned}$$

where the relaxation times in equations (3) are generated by the equations

$$\text{(5)} \qquad \begin{aligned} &\frac{1}{\left(\tau^{(m)}\right)^2} - \left(\frac{\lambda^{(m)}}{\hat{\tau}} + \frac{1+\beta}{\tilde{\tau}}\right)\frac{1}{\tau^{(m)}} + \frac{\lambda^{(m)}}{\hat{\tau}\tilde{\tau}} = 0, \\ &\lambda^{(m)} \;=\; 4\sin^2\frac{(2m-1)}{(2M+1)}\frac{\pi}{2}, \qquad m = 1, 2, \ldots, M, \end{aligned}$$

and $M$ is the number of lacunae in lacunar-canalicular series (Fig. 1). Typical anatomical feature for $M$, for mature osteon, is 4, 5 or 6.

The continual extrapolations of the discrete equations (3) are

(6)
$$P(u) = P_0 \sum_{m=1}^{M} C^m \left( \frac{\tau_1^m - \tilde{\tau}}{\tau_1^m - \tau_2^m} \exp\left(-\frac{t}{\tau_1^m}\right) + \right.$$
$$\left. + \frac{\tilde{\tau} - \tau_2^m}{\tau_1^m - \tau_2^m} \exp\left(-\frac{t}{\tau_2^m}\right)\right) \sin\frac{(2m-1)u\pi}{(2M+1)L},$$
$$\tilde{P}(u) = P_0 \sum_{m=1}^{M} C^m \left( \frac{\tau_1^m}{\tau_1^m - \tau_2^m} \exp\left(-\frac{t}{\tau_1^m}\right) - \right.$$
$$\left. - \frac{\tau_2^m}{\tau_1^m - \tau_2^m} \exp\left(-\frac{t}{\tau_2^m}\right)\right) \sin\frac{(2m-1)u\pi}{(2M+1)L},$$

where $u$ is the position point (the distance from Haversian canal). Consequently the lacunar-canalicular and microporosity pressures on the cement line (osteonal periphery is $u = (2M+1)L/2)$) are

(7)
$$P_{cement} = P_0 \sum_{m=1}^{M} C^m \left( \frac{\tau_1^m - \tilde{\tau}}{\tau_1^m - \tau_2^m} \exp\left(-\frac{t}{\tau_1^m}\right) + \right.$$
$$\left. + \frac{\tilde{\tau} - \tau_2^m}{\tau_1^m - \tau_2^m} \exp\left(-\frac{t}{\tau_2^m}\right)\right) \sin(2m-1)\frac{\pi}{2},$$
$$\tilde{P}_{cement} = P_0 \sum_{m=1}^{M} C^m \left( \frac{\tau_1^m}{\tau_1^m - \tau_2^m} \exp\left(-\frac{t}{\tau_1^m}\right) - \right.$$
$$\left. - \frac{\tau_2^m}{\tau_1^m - \tau_2^m} \exp\left(-\frac{t}{\tau_2^m}\right)\right) \sin(2m-1)\frac{\pi}{2}.$$

As typical case we shall chouse, in our osteonial model, five lacunae in series first connected with Haversian canal, which means $M = 5$. The constants $C^m$ are subjected to initial condition $(1)_3$. Consequently we have

(8) $$C^1 = 1,26, \quad C^2 = 0,4, \quad C^3 = 0,21, \quad C^4 = 0,12, \quad C^5 = 0,05.$$

Also because of the size of the test electrode in streaming potential measuring equipment [3], [10], [11] the results for the streaming potentials should

Table 1

| Data from | Model | $\hat{\tau}$ | $\tilde{\tau}$ | $\beta$ |
|---|---|---|---|---|
| Pienkowski [3] | Petrov and Pollack [9] | 0,02 | 1,1 | 1,2 |
| Sample BT3-90-7 | Kufahl and Saha [4] | 0,03 | — | 0,0 |
| Pienkowski [3] | Petrov and Pollack [9] | 0,03 | 2,2 | 1,1 |
| Sample BT3-90-8 | Kufahl and Saha [4] | 0,04 | — | 0,0 |
| Otter *et al.* [11] | Petrov and Pollack [9] | 0,05 | 2,1 | 1,6 |
| in vitro | Kufahl and Saha [4] | 0,09 | — | 0,0 |
| Otter *et al.* [11] | Petrov and Pollack [9] | 0,04 | 2,1 | 0,6 |
| in vivo | Kufahl and Saha [4] | 0,05 | — | 0,0 |

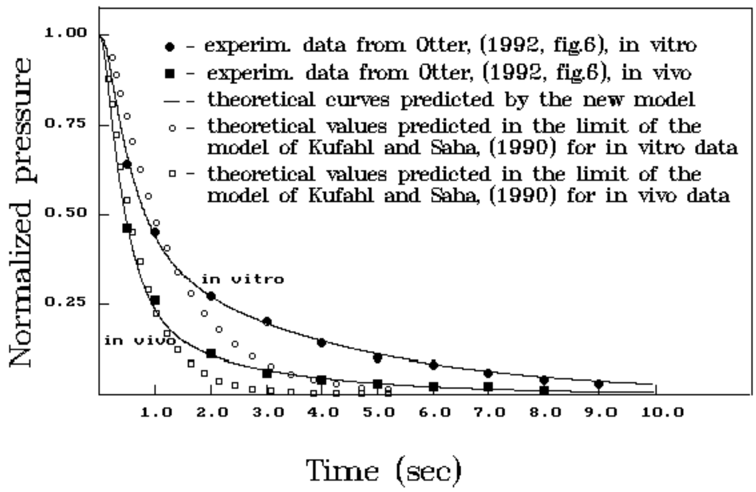


Fig. 3. Model predicted fluid pressure responses to step-function load and the least square approximations of the experimental curves with the theoretical model of Petrov and Pollack [9]

be compared to the fluid pressure in lacunar-canalicular compartment, but not to the fluid pressure in microporosity compartment, which is not accessible for the electrode. By the same size scale reason, topographically, all measurements should be concerning with respect to the osteonial cement line, but not to the oseonal inside. As it was mentioned before, the present mathematical model is dependent only on three parameter combinations, namely – $\hat{\tau}$, $\tilde{\tau}$, $\beta$. That is why it is convenient they to be used as fitting parameters for theoretical approaching to experimental decay curves. In Table 1 [9] are represented the respective values, obtained by least squares method – minimization of the sum of squares of the differences between the theoretical and experimental curve [10, 11]. The fitting ability of the model is demonstrated by Fig. 3 [9].

## 4. Only two relaxation times appear in all step type loading experiments

If we substitute the values for $\hat{\tau}$, $\tilde{\tau}$, $\beta$ processed for sample BT3-90-7 (Table 1), into (4) and $(8)_1$ we obtain

$$
\begin{aligned}
&\frac{P_{cement}}{P_0} = 0,36\exp\left(-\frac{t}{1,46}\right) + 0,64\exp\left(-\frac{t}{0,19}\right) - \\
&-0,01\exp\left(-\frac{t}{1,14}\right) - 0,43\exp\left(-\frac{t}{0,03}\right) + 0,0025\exp\left(-\frac{t}{1,11}\right) + \\
&+0,25\exp\left(-\frac{t}{0,01}\right) - 0,0018\exp\left(-\frac{t}{1,11}\right) - 0,18\exp\left(-\frac{t}{0,01}\right) + \\
&+0,0014\exp\left(-\frac{t}{1,11}\right) + 0,14\exp\left(-\frac{t}{0,01}\right).
\end{aligned}
\tag{9}
$$

It is of importance, in processing the experimental curves to omit all amplitude with magnitude of about a few percents or less with respect to the top value. Also it should be mention that the rise time at step loading, for the cited quasi static experiments, is about 0, 03 sec, which leads to not observability of all process components with decay time of the same or smaller value. Therefore, we have

$$
\frac{P_{cement}}{P_0} = 0,36\exp\left(-\frac{t}{1,46}\right) + 0,64\exp\left(-\frac{t}{0,19}\right). \tag{10}
$$

This result is in perfect accordance with the experimental data. The step loading type experimental studies of Pienkowski [3], Otter *at al.* [11]

and others clearly demonstrate two decay times. The same conclusion, after processing, could be done for all cited here relaxation type experimental curves of Pienkowsky [3] and Otter *et al.* [11].

For the micro-porosity on the cement line we may predict

$$\frac{\tilde{P}_{cement}}{P_0} = 1,46\exp\left(-\frac{t}{1,46}\right) - 0,19\exp\left(-\frac{t}{0,19}\right) - \tag{11}$$
$$-0,43\exp\left(-\frac{t}{1,14}\right) + 0,21\exp\left(-\frac{t}{1,11}\right).$$

Opposite to the case of lacunar-canalicular pressure relaxation, the theory predicts that the microporosity pressure relaxation is described by four relaxation times, however till to now such a experiment of measuring the microporosity pressure is not yet done.

## 5. Conclusions

First, it was demonstrated for relaxation type experiments that the model is capable of an excellent fit to the multi-time-constant experimental data using only three parameter combinations, namely $\hat{\tau}$, $\tilde{\tau}$, $\beta$ instead of ten anatomical parameters and physical constants.

Second, the model avoids the use of hypothetical assumptions for frozen state of the microporosity fluid and the existence of structured glycocalyx within canaliculus.

Third, the observation of only two relaxation times, at step type bone samples loading experiments, is explained quantitatively for first time in the literature.

## REFERENCES

[1] Piekarski, K., M. Munro. Transport Mechanism Operating between Blood Supply and Osteocytes in Long Bones. *Nature*, **269** (1977), No. **5623**, 80–82.

[2] Pollack, S. R., N. Petrov, R. Salzstein, G. Brankov, R. Blagoeva. An Anatomical Model for Streaming Potentials in Osteons. *J. Biomechanics*, **17**(1984), 627–636.

[3] Pienkowski, D. The Effect of Fluids on Stress Generated Potentials in Bone, PhD Thesis, University of Pennsylvania, University Microfilms International, Ann Arbor, Michigan, London, 1982.

[4] Kufahl, R. H., S. Saha. A Theoretical Model for Stress - Generated Fluid Flow in the Canaliculi-Lacunae Network in Bone Tissue. *J. Biomechanics*, **23**(1990), 171–180.

[5] Weinbaum, S., C. Cowin, Y. Zeng. A Model for the Excitation of Osteocytes by Mechanical Loading - Induced Lone Fluid Shear Stresses. *J. Biomechanics*, **27** (1994), 339–360.

[6] Zeng, Y., S. C. Cowin, S. Weinbaum. A Fiber Matrix Model for Fluid Flow and Streaming Potentials in the Canaliculi of an Osteon, *Annals of Biomedical Engineering*, **22**(1994), 280–292.

[7] Neuman, W. F., M. W. Neuman. In: The Chemical Dynamics of Bone Minerals, Chicago, University of Chicago Press, IL, 1958.

[8] [8] Dillaman, R. M. Movement of Ferritin in 2-Day-Old Chick Femur. *Anat. Rec.*, **209** (1984), 445–453.

[9] Petrov, N., S. R. Pollack. An Anatomical Model of Stress Induced Fluid Flow in Osteons, In: International Conference on Biorheology Proceeding, 18–22 October, 2000, Sofia, Bulgaria.

[10] Pienkowski, D., S. R. Pollack. The Origin of Stress Generated Potentials in Fluid Saturated Bone. *J. Orthop. Res.*, **1** (1983), 30–41.

[11] Otter, W. M., V. R. Palmieri, D. D. Wu, K. G. Seiz, L. A. Macginitie, G. V. B. Cochran. A Comparative Analysis of Streaming Potentials in Vivo and in Vitro. *J. Orth. Res.*, **10** (1992), 710–719.